Applied Catalysis B: Environmental 90 (2009) 368–379

Contents lists available at ScienceDirect

Applied Catalysis B: Environmental

journal homepage: www.elsevier.com/locate/apcatb

A thermogravimetric and FT-IR study of the reduction by H_2 of sulfated $Pt/Ce_xZr_{1-x}O_2$ solids

P. Bazin [a,*], O. Saur [a], F.C. Meunier [a], M. Daturi [a], J.C. Lavalley [a], A.M. Le Govic [b], V. Harlé [b], G. Blanchard [b,1]

[a] Laboratoire Catalyse et Spectrochimie, ENSICAEN, Université de Caen, CNRS, 6 Bd Maréchal Juin, F-14050 Caen, France
[b] Rhodia Recherches et Technologies, 52 rue de la Haie Coq, 93 308 Aubervilliers, France

ARTICLE INFO

Article history:
Received 21 January 2009
Received in revised form 13 March 2009
Accepted 16 March 2009
Available online 25 March 2009

Keywords:
Three-way catalysts
Oxygen storage capacity
Ceria–zirconia
Platinum
Sulfate
Sulfur dioxide
IR spectroscopy
Thermogravimetry

ABSTRACT

The nature, concentration and reducibility by H_2 of sulfate species formed from SO_2 oxidation were studied over a range of $Pt/Ce_xZr_{1-x}O_2$ catalysts using infrared spectroscopy and thermogravimetry. Ionic sulfates were formed over ceria and Ce-containing catalysts, even at high Zr content. The sample-specific surface area, the presence of platinum and the zirconium proportion affected the rate and extent of formation of sulfate in the bulk of the materials. Sulfate reduction by H_2 first occurred at the $Ce_xZr_{1-x}O_2$ surface. Bulk-like S-containing species subsequently migrated towards the surface to continuously replace surface sulfates removed by the reduction. The temperature required for sulfate migration as well as that necessary for sulfate reduction increased with the Zr content. The amount of stored sulfur is closely linked to the specific surface area of the sample. Finally, we have clearly shown that thermogravimetry was an appropriate technique for evaluating the oxygen storage capacity (OSC) of sulfated ceria–zirconia mixed oxides, despite the additional complexity due to the presence of sulfate compounds and various reduced S-species that can be formed during sample reduction.

1. Introduction

Ceria is an important component of three-way catalysts (TWCs), in part because of its large oxygen storage capacity (OSC) [1,2]. Ceria is being replaced by mixed oxides based on cerium and zirconium in recent TWCs formulations. The presence of zirconium increases the thermal stability of the oxide at high temperatures [3] and the OSC [4,5]. Platinum is also a standard component of TWCs and is used for the oxidation of CO and hydrocarbons [6] and for NO conversion [7]. A major difficulty for automotive exhaust control arises from the presence of organo-sulfur compounds in most fossil fuels. These compounds are oxidized during the combustion process and the sulfur oxides formed can poison the TWCs. More dramatic problems are encountered in the case of diesel or Lean burn engines, in which the TWCs are replaced by NO_x control systems often based on the NO_x-traps. Highly stable sulfates are formed on the NO_x storage sites and a periodic reactivation achieved at high temperatures is required to regenerate the poisoned trap. Therefore, the results obtained from this study directly regard NO_x-trap catalyst regeneration, as well as the surface behavior of sulfated supports as recently reported for low temperature H_2-SCR [8].

Our laboratory previously reported IR spectroscopic and thermogravimetric studies of the sulfation (using a $SO_2 + O_2$ gas stream) of ceria, zirconia and a ceria–zirconia mixed oxide (Ce/Zr = 64/36, atomic ratio) and of the reduction of the same materials under H_2 [9–11]. The IR work highlighted the formation of two kinds of sulfate species: (i) sulfates with sulfur–oxygen bonds having a covalent character, therefore assigned to surface species and (ii) sulfates showing ionic bonds, being the fingerprint of bulk species. The ionic species were likely formed within the bulk of the materials following the diffusion of SO_x species from the surface. Only surface sulfate species were observed on zirconia, even in the presence of platinum, while bulk-like sulfates were also formed in the case of ceria and the $Ce_{0.64}Zr_{0.36}O_2$ mixed oxide [11]. Our previous work showed that platinum favored the reducibility by H_2 of both sulfate species on all studied catalysts and that sulfates on $Ce_{0.64}Zr_{0.36}O_2$ were more easily reduced than sulfates on pure ceria. This result is important: it stressed that mixed oxides could potentially be more easily regenerated than pure ceria. A mechanism for sulfate formation versus temperature was proposed. First, sulfite species were formed at low temperatures. Second, surface sulfate species appeared at the expense of sulfite species and, finally, the diffusion of surface sulfate into the bulk of the sample occurred.

* Corresponding author. Fax: +332 31 45 28 22.
E-mail address: philippe.bazin@ensicaen.fr (P. Bazin).
[1] Current address: PSA, Centre Technique de Velizy, France.

0926-3373/$ – see front matter.
doi:10.1016/j.apcatb.2009.03.016

Luo and Gorte reported that the quantity of sulfates formed at 673 K increased linearly with the Ce content in the case of Pd supported on ceria–zirconia mixed oxides [12]. These authors concluded that it was very difficult to determine the oxygen storage capacity (OSC) of sulfated ceria–zirconia mixed oxides, in particular by pulse-reactor method, due to the presence of SO_x groups, which led to an apparent increase of the OSC. In the present paper, we compare the nature, concentration and hydrogen reducibility of sulfate species formed from SO_2 oxidation on a series of $Ce_xZr_{1-x}O_2$ catalysts supported platinum, in order to evaluate the influence of Zr addition to ceria on sulfur storage. This work gives a more in-depth analysis of the structure–SO_x storage relationship and, in particular, shows that it is possible to determine accurately the OSC of Ce–Zr mixed oxides in a simple and straightforward manner, despite the presence of reducible SO_x groups.

2. Experimental

2.1. Materials

Ceria (CeO_2), zirconia (ZrO_2) and $Ce_xZr_{1-x}O_2$ mixed oxides were obtained by a Rhodia proprietary process via nitrate precursors [13] and calcined at 773 K. A solution of hexachloroplatinic was used as platinum precursor. After several washing treatments, the impregnated material obtained were dried in an oven at 393 K and calcined in a muffle furnace at 773 K. Elemental analysis showed that the residual chlorine content in the sample was below the detection limit. The Pt loading was 0.5% (weight percentage). A second series of samples were obtained by an additional thermal treatment at 1173 K. This series of samples calcined at 1173 K will be denoted by the –C suffix and also referred to as "aged" samples. The specific surface areas of the oxides were measured by nitrogen adsorption, using the BET method and are reported in Table 1.

2.2. Infrared study

The samples were pressed in a die set of 16 mm of diameter into self-supported wafers of approximately 10 mg cm^{-2} and treated *in situ* in a quartz cell equipped with KBr windows for the infrared studies. An assembly connected to the IR cell containing a calibrated volume (of ca. 1.5 cm^3) delimited by two valves and a pressure gauge was used to quantify precisely the amount of gaseous species introduced in the cell. IR spectra were recorded with a Nicolet Magna 550 FTIR spectrometer (operating at a resolution of 4 cm^{-1}; 64 scans/spectrum) after quenching the sample to room temperature (RT). The spectra were treated using the OMNIC® software. In order to decrease signal due to ambient water and carbon dioxide, the spectrometer and the sample compartment were purged with H_2O and CO_2-free air produced by a Floxal purge gas generator.

All samples were submitted to a standard cleaning pre-treatment with a view to eliminate impurities. The cleaning procedure consisted in calcining at 723 K under dioxygen for 2 h and then evacuating ($\sim 10^{-4}$ Pa) at the same temperature.

The materials were exposed to 600 μmol of SO_2 per gram of sample (corresponding to about 2 wt% sulfur) and a large excess of O_2 ($P \approx 6.5$ kPa at equilibrium) directly in the cell to study sample sulfation. The solids were then heated up stepwise to 323, 423, 523, 623 and 723 K. The samples obtained by this treatment were identified using the –S suffix.

Sulfated samples were first evacuated ($\sim 10^{-4}$ Pa) at 723 K for the study of sulfate reduction versus temperature. Subsequently, a large excess of H_2 (ca. 13 kPa at equilibrium) was introduced in the cell at RT. Finally the wafers were heated for 30 min stepwise to 323, 423, 523, 623 and 723 K, followed by an evacuation for 15 min at each temperature.

2.3. Thermogravimetric study

A McBain thermobalance was used for gravimetric measurements. The powders (approximately 400 mg) were pressed, activated and sulfated using the same procedure as that used for the IR study. The temperature was increased from RT to 723 K (using a temperature ramp of 0.5 K min^{-1}) and then kept at 723 K until a constant value was obtained for the sample weight. A large excess of H_2 ($P \sim 13$ kPa) was introduced at RT in the thermobalance to study the sulfate reduction and the sample was then heated up to higher temperatures using a temperature ramp of 0.5 K min^{-1}.

3. Results and discussion

3.1. Sulfation

3.1.1. Nature of the sulfate species

We have reported in previous work that the presence of platinum does not modify the nature of the sulfate species present on ceria, zirconia and ceria–zirconia mixed oxides [10,11]. Therefore, only the results regarding the nature of the sulfate

Table 1
Main characteristics of samples.

Samples		Atomic ratio		Weight ratio		Pt loading (weight %)	Surface area ($m^2\ g^{-1}$)
		Ce (atomic %)	Zr (atomic %)	CeO_2 (weight %)	ZrO_2 (weight %)		
Calcination at 773 K	CeO_2	100	0	100	0	0	170
	$Ce_{0.63}Zr_{0.37}O_2$	63	37	70	30	0	137
	$Ce_{0.50}Zr_{0.50}O_2$	50	50	58	42	0	106
	$Ce_{0.15}Zr_{0.85}O_2$	15	85	20	80	0	97
	ZrO_2	0	100	0	100	0	40
	Pt/CeO_2	100	0	100	0	0.5	147
	$Pt/Ce_{0.63}Zr_{0.37}O_2$	63	37	70	30	0.5	107
	$Pt/Ce_{0.50}Zr_{0.50}O_2$	50	50	58	42	0.5	96
	$Pt/Ce_{0.15}Zr_{0.85}O_2$	15	85	20	80	0.5	91
	Pt/ZrO_2	0	100	0	100	0.5	40
Calcination at 1173 K	CeO_2–C	100	0	100	0	0	26
	$Ce_{0.63}Zr_{0.37}O_2$–C	63	37	70	30	0	37
	$Ce_{0.50}Zr_{0.50}O_2$–C	50	50	58	42	0	33
	Pt/CeO_2–C	100	0	100	0	0.5	22
	$Pt/Ce_{0.63}Zr_{0.37}O_2$–C	63	37	70	30	0.5	32
	$Pt/Ce_{0.50}Zr_{0.50}O_2$–C	50	50	58	42	0.5	30
	$Pt/Ce_{0.15}Zr_{0.85}O_2$–C	15	85	20	80	0.5	40

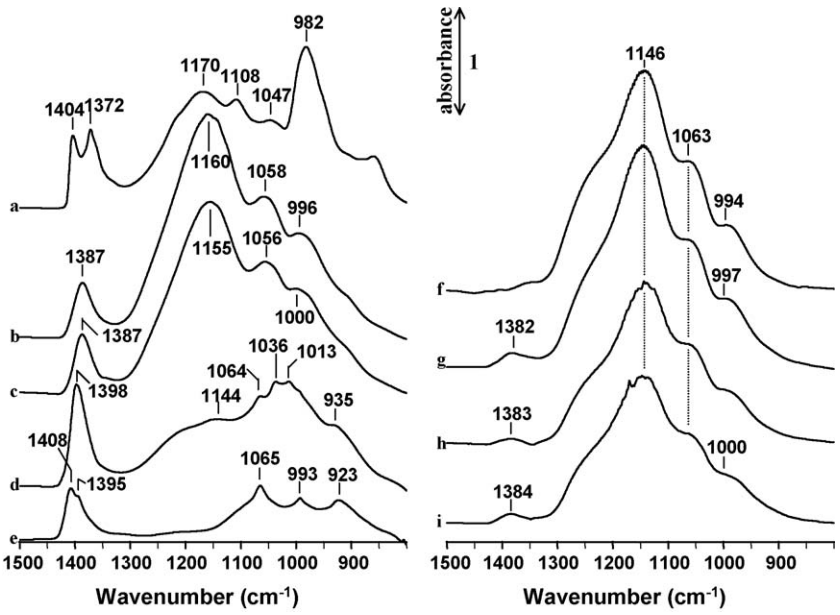

Fig. 1. IR spectra of sulfate species formed by heating 600 μmol g^{-1} of SO_2 in an excess of O_2 (6.5 kPa) at 673 K during 12 h, followed by an evacuation at the same temperature on various samples: (a) CeO_2, (b) $Ce_{0.63}Zr_{0.37}O_2$, (c) $Ce_{0.50}Zr_{0.50}O_2$, (d) $Ce_{0.15}Zr_{0.85}O_2$, (e) ZrO_2, (f) CeO_2–C, (g) $Ce_{0.63}Zr_{0.37}O_2$–C, (h) $Ce_{0.50}Zr_{0.50}O_2$–C, (i) $Pt/Ce_{0.15}Zr_{0.85}O_2$–C.

species observed on the Pt-free samples are shown here (excepted for $Pt/Ce_{0.15}Zr_{0.85}O_2$–C). The spectra of the sulfate species formed on CeO_2, ZrO_2 and the mixed oxides $Ce_{0.63}Zr_{0.37}O_2$, $Ce_{0.50}Zr_{0.50}O_2$, $Ce_{0.15}Zr_{0.85}O_2$ after treatment at 673 K with SO_2 (600 μmol g^{-1}) and O_2 ($P \sim 6.5$ kPa) and evacuation at the same temperature are reported in Fig. 1. The spectra on the left side of the figure correspond to the samples calcined at 773 K, while those on the right side relates to the powders treated at 1173 K. Only surface sulfate species were formed on zirconia (spectrum 1e). The bands at 1395 and 1408 cm^{-1} can be assigned in fact to the ν(S=O) vibrations of surface sulfate [14] and surface pyrosulfates ($S_2O_7^{2-}$) species, respectively. The bands observed at 1065, 993 and 923 cm^{-1} were due to ν(S–O) vibrations of these species. On the contrary, both surface and bulk sulfate species were observed on ceria (spectrum 1a): (i) surface sulfate species (ν(S=O) vibrations in the range 1400–1350 cm^{-1}) and (ii) ionic species located in the bulk or subsurface of the sample (broad band near 1150 cm^{-1}) [10,11]. Surface and bulk sulfate species were also observed in the case of the mixed oxides: surface species with bands at 1387 cm^{-1} for both $Ce_{0.63}Zr_{0.37}O_2$ and $Ce_{0.50}Zr_{0.50}O_2$ (Fig. 1c) and at 1398 cm^{-1} for $Ce_{0.15}Zr_{0.85}O_2$ (Fig. 1d), while the bands of bulk-like species were located near 1160 cm^{-1}. These observations indicate that ceria retained the ability to form ionic sulfates even in the form of a mixed oxide with high zirconium contents. The spectra of sulfated $Ce_{0.50}Zr_{0.50}O_2$ and $Ce_{0.63}Zr_{0.37}O_2$ were very similar, but that of $Ce_{0.15}Zr_{0.85}O_2$ presented a much weaker ionic band, which was shifted to lower wavenumbers. This result indicates that the amount of bulk-like species was less important on the $Ce_{0.15}Zr_{0.85}O_2$ sample.

The IR spectra of the sulfated samples calcined at 1173 K (spectra Fig. 1, f–i) were mainly composed of a broad band centered at 1146 cm^{-1}, which was associated with ionic sulfate species. The amount of surface sulfate species was low considering the weak intensity of the peak located near 1383 cm^{-1}. The intensity of the complex feature centered at 1146 cm^{-1} seemed to decrease with the increasing of zirconium amount. This leads to suppose that the addition of zirconia into ceria limits sulfation in the bulk of the oxide. Only surface sulfates (hence non-ionic) are formed over zirconia [10]. Therefore, the quantity of sulfate species formed is directly related to the surface area. A calcination at 1173 K of ZrO_2 meanly led to a decrease of the surface area, therefore to a decrease of the amount of surface sulfates.

3.1.2. Formation of sulfate species on Pt-free oxides

Fig. 2A shows the mass changes recorded over the Pt-free oxides (which were initially calcined at 773 K), heated up to 730 K at a rate of 0.5 K min^{-1} in the thermobalance in the presence of SO_2 (600 μmol g^{-1}) and O_2 ($P \sim 6.5$ kPa). The weight of the CeO_2 (curve a) and $Ce_{0.63}Zr_{0.37}O_2$ (curve b) materials gradually increased up to 573 K, temperature at which the sample mass remained constant. This point corresponded to the total conversion of the gas-phase SO_2 contained in the chamber into sulfate species on the samples. In the case of $Ce_{0.50}Zr_{0.50}O_2$ sample (curve c), an inflection point was observed at around 473 K. This phenomenon was more evident in the case of the $Ce_{0.15}Zr_{0.85}O_2$ material (curve d), for which a plateau was observed.

Fig. 2B shows the corresponding mass changes for the Pt-free samples that were initially calcined at 1173 K. After an initial fast uptake of a moderate value, the mass gain remained unchanged constant up to ca. 500 K, before subsequently rising again. This complex behavior is attributed to surface area effects [10]. Only surface species (sulfite and then sulfate) were formed at low temperature, while bulk-like sulfate also appeared above 473 K.

The amounts of sulfate species formed by oxidation of the SO_2 present in the IR cell (600 μmol g^{-1}) in the presence of an excess of oxygen are reported in Table 2. The values were recorded when a steady mass signal was obtained at 723 K. A mass uptake of 48 mg g^{-1} of sample should be expected if all the SO_2 present was oxidized to SO_3 and adsorbed on surface oxygen atoms (i.e. $SO_2 + (1/2)O_2 + (O^{2-})_{lattice} \rightarrow SO_4^{2-}$). The mass gain measured in the cases of the CeO_2, $Ce_{0.63}Zr_{0.37}O_2$ and $Ce_{0.50}Zr_{0.50}O_2$ samples calcined at 773 K, which exhibited a rather large specific surface area (Table 1), were essentially identical to this maximum uptake value of 48 mg g^{-1} (Table 2). On the contrary, only a mass gain of 42.5 mg g^{-1} was obtained in the case of the $Ce_{0.15}Zr_{0.85}O_2$ sample. This lower uptake is consistent with the IR data showing fewer ionic sulfate species formed on the $Ce_{0.15}Zr_{0.85}O_2$ mixed oxide (Fig. 1e).

The results regarding the samples calcined at 1173 K indicated that only a fraction of the SO_2 present was converted into sulfate

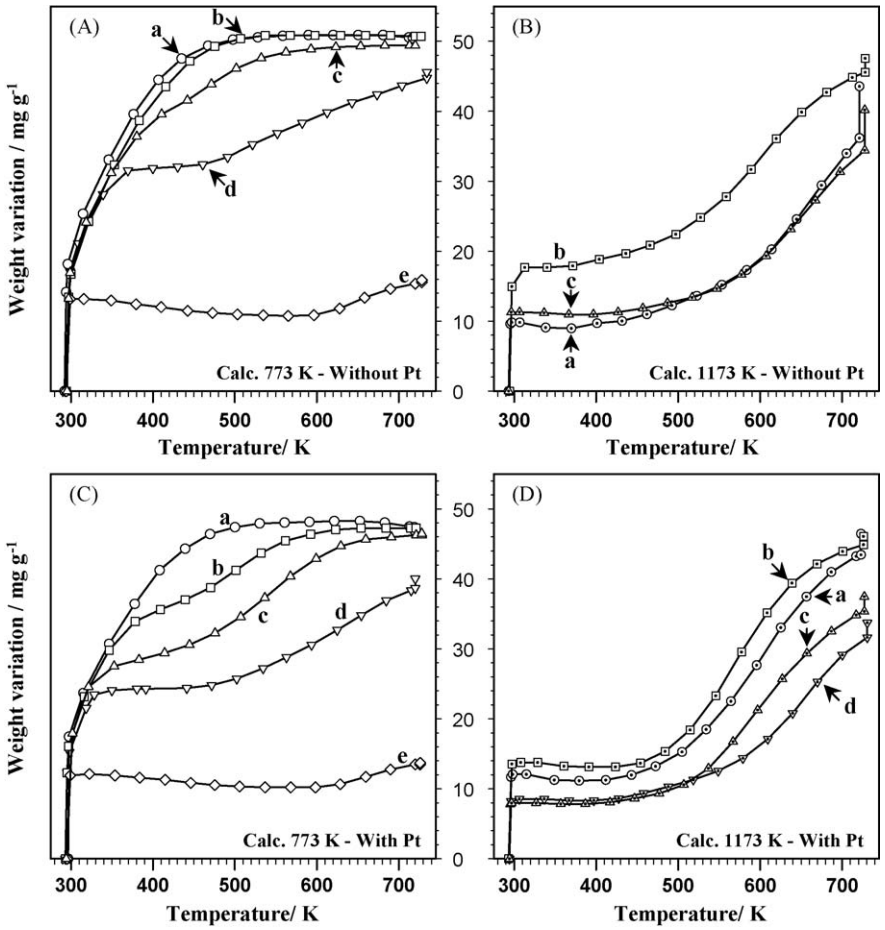

Fig. 2. Mass gain of various samples heated from 298 K to 723 K under SO_2 (600 μmol g^{-1}) and O_2 (6.5 kPa)—A: (a) CeO_2, (b) $Ce_{0.63}Zr_{0.37}O_2$, (c) $Ce_{0.50}Zr_{0.50}O_2$, (d) $Ce_{0.15}Zr_{0.85}O_2$, (e) ZrO_2; B: (a) CeO_2–C, (b) $Ce_{0.63}Zr_{0.37}O_2$–C, (c) $Ce_{0.50}Zr_{0.50}O_2$–C; C: (a) Pt/CeO_2, (b) $Pt/Ce_{0.63}Zr_{0.37}O_2$, (c) $Pt/Ce_{0.50}Zr_{0.50}O_2$, (d) $Pt/Ce_{0.15}Zr_{0.85}O_2$, (e) Pt/ZrO_2; D: (a) Pt/CeO_2–C, (b) $Pt/Ce_{0.63}Zr_{0.37}O_2$–C, (c) $Pt/Ce_{0.50}Zr_{0.50}O_2$–C, (d) $Pt/Ce_{0.15}Zr_{0.85}O_2$–C.

Table 2
Quantitative values of thermogravimetric measurements.

Samples	Sulfation[a]		H_2 Red.[b]		O_2 re-oxidation[d]		Oxide reduction[e]	
	m_1[c] (mg g^{-1})	Sulfate storage (μmol g^{-1})	m_2[c] (mg g^{-1})	m_1–m_2 (mg g^{-1})	m_3[c] (mg g^{-1})	Sulfur storage (μmol g^{-1})	O_{atomic} destorage (μmol g^{-1})	x in $CeZrO_x$
CeO_2	48.0	600	+1.1	46.9	36.2	453	837	1.86
$Ce_{0.63}Zr_{0.37}O_2$	48.2	602	−8.4	56.6	29.1	364	1254	1.81
$Ce_{0.50}Zr_{0.50}O_2$	48.2	603	−10.7	58.9	25.0	313	1295	1.81
$Ce_{0.15}Zr_{0.85}O_2$	42.5	531	−3.0	45.5	13.1	164	514	1.93
ZrO_2	13.7	171	0.1	13.6	1.1	14	–	–
Pt/CeO_2	45.9	573	+1.8	44.1	34.5	431	752	1.87
$Pt/Ce_{0.63}Zr_{0.37}O_2$	45.0	562	−8.8	53.8	27.8	347	1245	1.81
$Pt/Ce_{0.50}Zr_{0.50}O_2$	43.5	544	−10.9	54.4	21.6	270	1219	1.82
$Pt/Ce_{0.15}Zr_{0.85}O_2$	36.7	459	−5.8	42.5	9.9	124	608	1.92
Pt/ZrO_2	12.9	161	0.2	12.7	1.5	19	–	–
CeO_2–C	42.4	530	−0.4	42.8	7.4	92	163	1.97
$Ce_{0.63}Zr_{0.37}O_2$–C	45.1	564	−7.2	52.3	14.2	178	803	1.88
$Ce_{0.50}Zr_{0.50}O_2$–C	38.2	478	−8.9	47.1	10.4	130	818	1.88
Pt/CeO_2–C	45.1	564	+0.8	44.3	12.3	154	255	1.96
$Pt/Ce_{0.63}Zr_{0.37}O_2$–C	44.3	553	−5.8	50.1	14.1	176	716	1.89
$Pt/Ce_{0.50}Zr_{0.50}O_2$–C	34.8	435	−8.7	43.5	7.4	93	727	1.89
$Pt/Ce_{0.15}Zr_{0.85}O_2$–C	30.9	386	−6.2	37.1	3.8	48	487	1.94

[a] Sulfation by SO_2 (600 μmol g^{-1}) and O_2 (6.5 kPa), values have been determined when no mass variation is recorded at 723 K.
[b] Reduction by H_2 (13 kPa), values have been determined when no mass variation is recorded at 773 K.
[c] See Fig. 11.
[d] Re-oxidation under O_2 atmosphere at 673 K after the H_2 treatment.
[e] Oxide reduction evaluated after the H_2 treatment of sulfated sample.

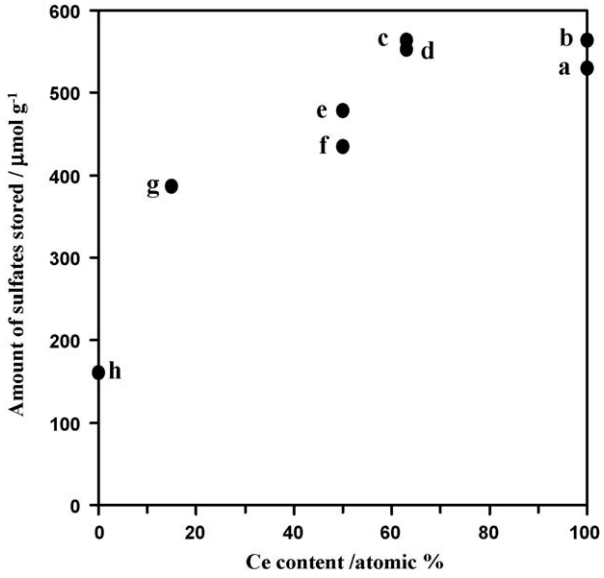

Fig. 3. Amount of sulfate stored on various samples at saturation versus the cerium content: (a) CeO_2–C, (b) Pt/CeO_2–C, (c) $Ce_{0.63}Zr_{0.37}O_2$–C, (d) Pt/$Ce_{0.63}Zr_{0.37}O_2$–C, (e) $Ce_{0.50}Zr_{0.50}O_2$–C, (f) Pt/$Ce_{0.50}Zr_{0.50}O_2$–C, (g) Pt/$Ce_{0.15}Zr_{0.85}O_2$–C and (g) Pt/ZrO_2.

species (Table 2). Interestingly, the mass gain was higher on the 26 $m^2\ g^{-1}$ CeO_2–C sample (i.e. 42.4 mg g^{-1}) than that observed on the 33 $m^2\ g^{-1}$ $Ce_{0.50}Zr_{0.50}O_2$–C (i.e. 38.2 mg g^{-1}). This observation indicates that the presence and concentration of zirconium are the main parameters influencing the sulfation process, and not the sample surface area (note: the migration of SO_x into the bulk of the mixed oxide is proposed as the rate determining step). On similar materials, Luo et al. suggested that sulfate species were associated with individual metal cations and that the quantity of sulfates formed at 673 K increased linearly with the Ce content [12]. No IR bands due to the presence of segregated sulfate ceria and sulfated zirconium were observed in the mixed oxides reported in our study (bands at around 1404 and 1372 cm^{-1} would be expected otherwise on the spectra of $Ce_{0.63}Zr_{0.37}O_2$–S, Fig. 1b). This result indicates that surface sulfates were not associated with a single metal cation, particularly in the case of cerium. For samples saturated by sulfates (mainly samples calcined at 1173 K), the amount of sulfate stored on mixed oxides did not vary linearly with the Ce content (Table 2 and Fig. 3).

3.1.3. Formation of sulfate species on Pt-containing oxides

The mass variations observed over the Pt-containing oxides heated from room temperature to 723 K (at a ramp of 0.5 K min^{-1}) under SO_2 (600 µmol g^{-1}) and O_2 ($P \sim 6.5$ kPa) are presented in Fig. 2C and 2D. The amount of stored sulfates was similar to that obtained without platinum (Table 2). However, the stored amount was somewhat lower in the case of the Pt-containing samples. This is probably due to a surface area effect. Therefore, the noble metal did not alter the capacity of the sample to store sulfates. The samples containing zirconium also lead to lower bulk-like sulfate concentrations. The mass gain curves versus temperature for samples with Pt (Fig. 2C and D) and without Pt (Fig. 2A and B) were similar, stressing that the kinetic of sulfation were mostly unchanged by the presence of the metal. The minor differences observed (e.g. breaking of slope near 373 K) were mainly due to specific surface area effects. The catalysts calcined at 1173 K were characterized by curves with a plateau between 298 and 473 K followed by a mass gain. While the value of this plateau was related to the specific surface area, the subsequent mass gain profile was different from one oxide to another.

3.1.4. Rate of sulfate uptake

The derivatives of mass gain curves for samples calcined at 1173 K were calculated with the aim to study in more details the relationship between sulfate formation and sample properties (Fig. 4). The comparison of the mass derivatives for the materials with and without Pt, in particular for CeO_2–C (Fig. 4A), $Ce_{0.63}Zr_{0.37}O_2$–C (Fig. 4B) and $Ce_{0.50}Zr_{0.50}O_2$–C (Fig. 4C), revealed that the mass variation was somewhat greater for Pt-supporting catalysts. The plots related to the Pt catalysts presented a maximum ca. 60 K lower than that of the Pt-free samples. Platinum appeared to favor the sulfate migration towards the bulk. Primet and colleagues [15] have observed a promoting effect of platinum for SO_2 oxidation on alumina, the oxidation in presence of Pt taking place at lower temperatures ($\Delta T \sim 150$ K) than that observed on pure oxide. Duprez and co-workers have shown that metals such as rhodium and platinum speed up significantly the isotopic exchange $^{18}O \rightarrow {}^{16}O$ of O_2 with the support [16–18]. This was explained by a spillover phenomenon of the oxygen coming from the metal particle towards the support. Also in our case, a spillover of oxygen from platinum to CeO_2 could increase the surface sulfation by an easier formation of SO_3. Surface sulfates would then move towards the bulk of the oxide. This migration has been evidenced in several cases [10,11], even if no investigation has yet been carried out on the elementary steps leading to sulfate diffusion. The situation remains the same whatever S-containing species is actually migrating, e.g. sulfate, sulfite, SO_2 or even bare sulfur. To our knowledge this is still an open question, difficult to answer, which would deserve an entire dedicated study. We have not observed any effect that could indicate that Pt facilitated sulfate migration towards the bulk for sample calcined at low temperature (773 K) presenting high

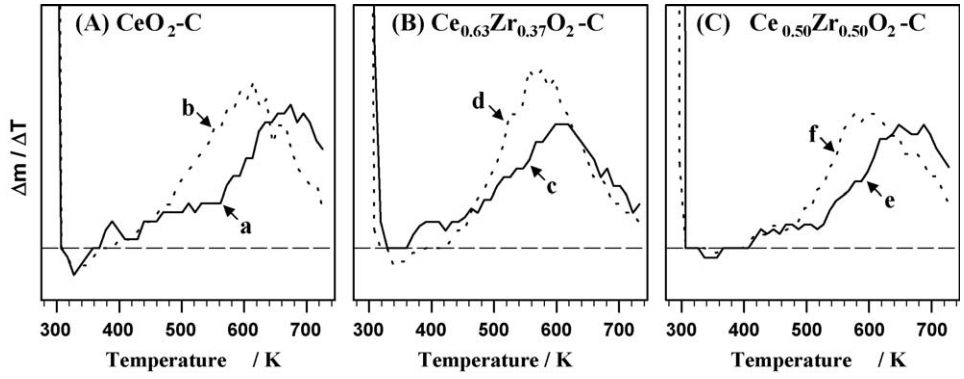

Fig. 4. Derivative of weight variation curves reported in Fig. 2—A: (a) CeO_2–C, (b) Pt/CeO_2–C; B: (c) $Ce_{0.63}Zr_{0.37}O_2$–C, (d) Pt/$Ce_{0.63}Zr_{0.37}O_2$–C; C: (e) $Ce_{0.50}Zr_{0.50}O_2$–C, (f) Pt/$Ce_{0.50}Zr_{0.50}O_2$–C.

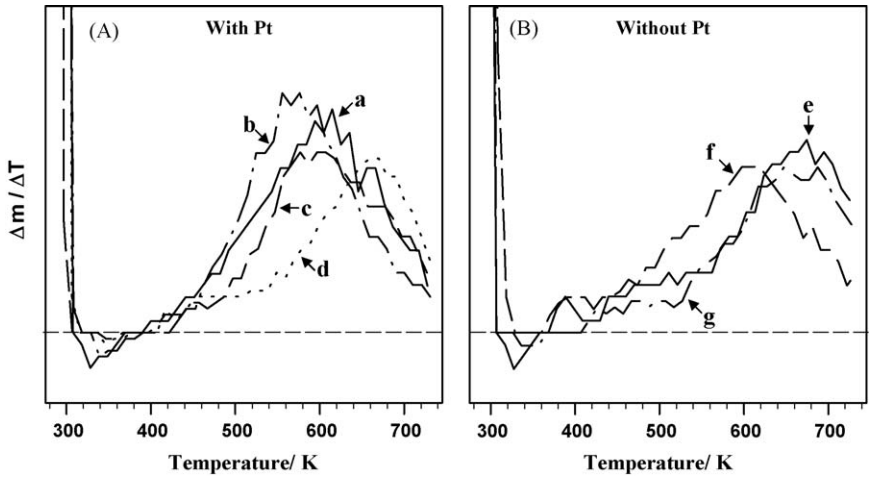

Fig. 5. Derivative of weight variation curves reported in Fig. 2—A: (a) Pt/CeO_2–C, (b) $Pt/Ce_{0.63}Zr_{0.37}O_2$–C, (c) $Pt/Ce_{0.50}Zr_{0.50}O_2$–C, (d) $Pt/Ce_{0.15}Zr_{0.85}O_2$–C; B: (e) CeO_2–C, (f) $Ce_{0.63}Zr_{0.37}O_2$–C, (g) $Ce_{0.50}Zr_{0.50}O_2$–C.

surface areas. The effect of the surface area on the migration is more important in comparison to the platinum effect.

The analysis of derivative curves reported in Fig. 5A shows different maxima for the various Pt-containing samples calcined at 1173 K. The maxima are observed at ~613 K, ~573 K, ~593 K and ~663 K for Pt/CeO_2–C (22 $m^2\ g^{-1}$), $Pt/Ce_{0.63}Zr_{0.37}O_2$–C (32 $m^2\ g^{-1}$), $Pt/Ce_{0.50}Zr_{0.50}O_2$–C (30 $m^2\ g^{-1}$) and $Pt/Ce_{0.15}Zr_{0.85}O_2$–C (40 $m^2\ g^{-1}$), respectively. The first conclusion arising from this result is that the higher the content of zirconium in the mixed oxide, the higher the temperature of the derivative maximum. The addition of zirconium appeared to decrease the mobility of surface sulfates towards the bulk of the oxide. However, the curve corresponding to Pt/CeO_2–C

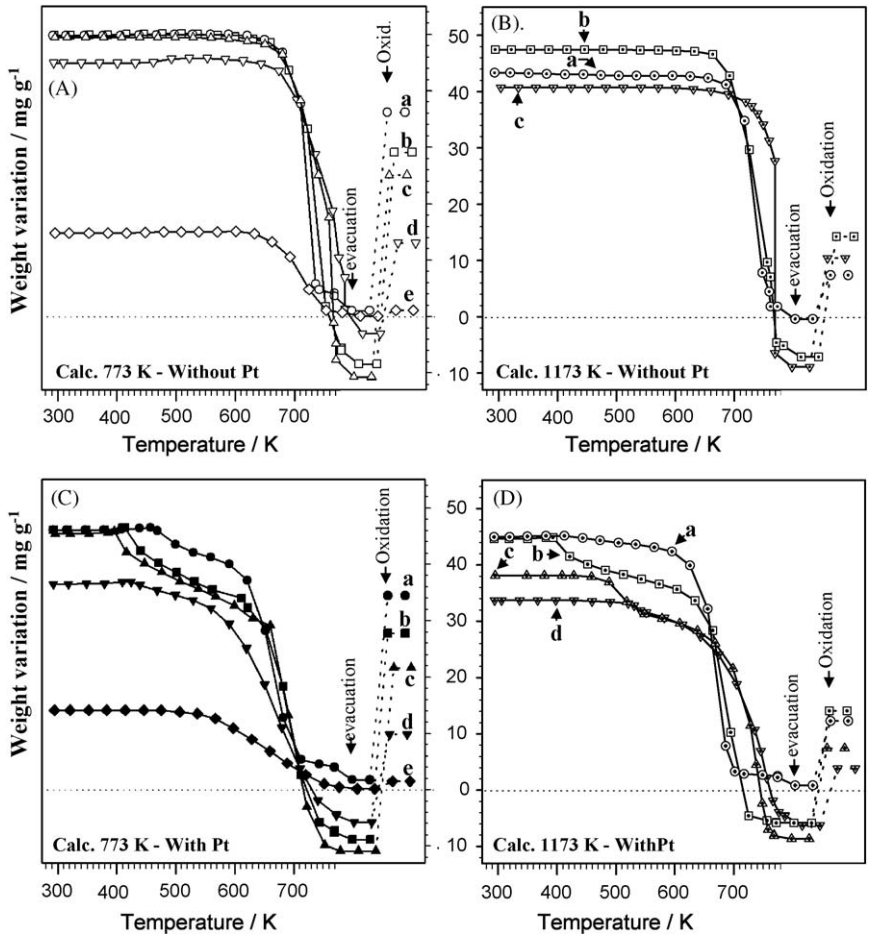

Fig. 6. Variation of the weight of various sulfated samples (heating of SO_2 (600 μmol g^{-1}) with O_2 (6.5 kPa) at 723 K) under H_2 atmosphere (13 kPa) from 298 to 773 K, then an evacuation and a re-oxidation under O_2 atmosphere at 673 K have been performed. A: (a) CeO_2, (b) $Ce_{0.63}Zr_{0.37}O_2$, (c) $Ce_{0.50}Zr_{0.50}O_2$, (d) $Ce_{0.15}Zr_{0.85}O_2$, (e) ZrO_2; B: (a) CeO_2–C, (b) $Ce_{0.63}Zr_{0.37}O_2$–C, (c) $Ce_{0.50}Zr_{0.50}O_2$–C; C: (a) Pt/CeO_2, (b) $Pt/Ce_{0.63}Zr_{0.37}O_2$, (c) $Pt/Ce_{0.50}Zr_{0.50}O_2$, (d) $Pt/Ce_{0.15}Zr_{0.85}O_2$, (e) Pt/ZrO_2; D: (a) Pt/CeO_2–C, (b) $Pt/Ce_{0.63}Zr_{0.37}O_2$–C, (c) $Pt/Ce_{0.50}Zr_{0.50}O_2$–C, (d) $Pt/Ce_{0.15}Zr_{0.85}O_2$–C.

(Fig. 5Aa) presents a maximum at higher temperature than that of $Pt/Ce_{0.63}Zr_{0.37}O_2$–C (curve 5Ab). In this case, the main factor limiting the migration inside Pt/CeO_2–C was most likely the low surface area. In fact the global rate of diffusion of a surface species towards the bulk is proportional to the concentration of the species on the surface. The latter then depends on the number density of sites (sites/m^2) that accommodate the diffusing species, since the SO_2 partial pressure was kept constant for all the experiments. All these observations relative to the samples with Pt calcined at 1173 K can be made for all the other samples (Fig. 5B).

3.2. Reduction of sulfates by H_2

3.2.1. Reduction of ZrO_2–S

Fig. 6Ae shows the mass variations of sulfated ZrO_2 (noted ZrO_2–S) in presence of H_2 ($P \sim 13.3$ kPa) in the range of temperatures 300–773 K. A mass loss of about 13.6 mg g^{-1} was observed between 633 and 773 K, corresponding to the overall concentration of sulfate species initially formed on the sample. The maximum of mass variation was at 723 K.

Infrared spectra of ZrO_2–S recorded in presence of hydrogen ($P \sim 13.3$ kPa) at various temperatures between 323 and 723 K (30 min for each temperature) are reported in Fig. 7Aa–i. The subtractions of two consecutive spectra are presented Fig. 7Aj–q. The sulfated sample (spectrum 7Aa) showed two bands at 1404 and 1395 cm^{-1} due to ν(S=O) vibration of pyrosulfate ($S_2O_7^{2-}$) and surface sulfate species (SO_4^{2-}), respectively [14,19–22]. In the 323–623 K temperature range (spectra 7Ab–e and j–m), no significant modification occurred. The intensity of the peaks associated with sulfate species decreased after H_2 treatment at 723 K. Firstly, the intensity of the band at 1409 cm^{-1} due to pyrosulfate species (spectrum n) decreased, then the band associated to surface monosulfate species decreased (spectra o, p and q). Therefore, pyrosulfate species were easier to reduce with

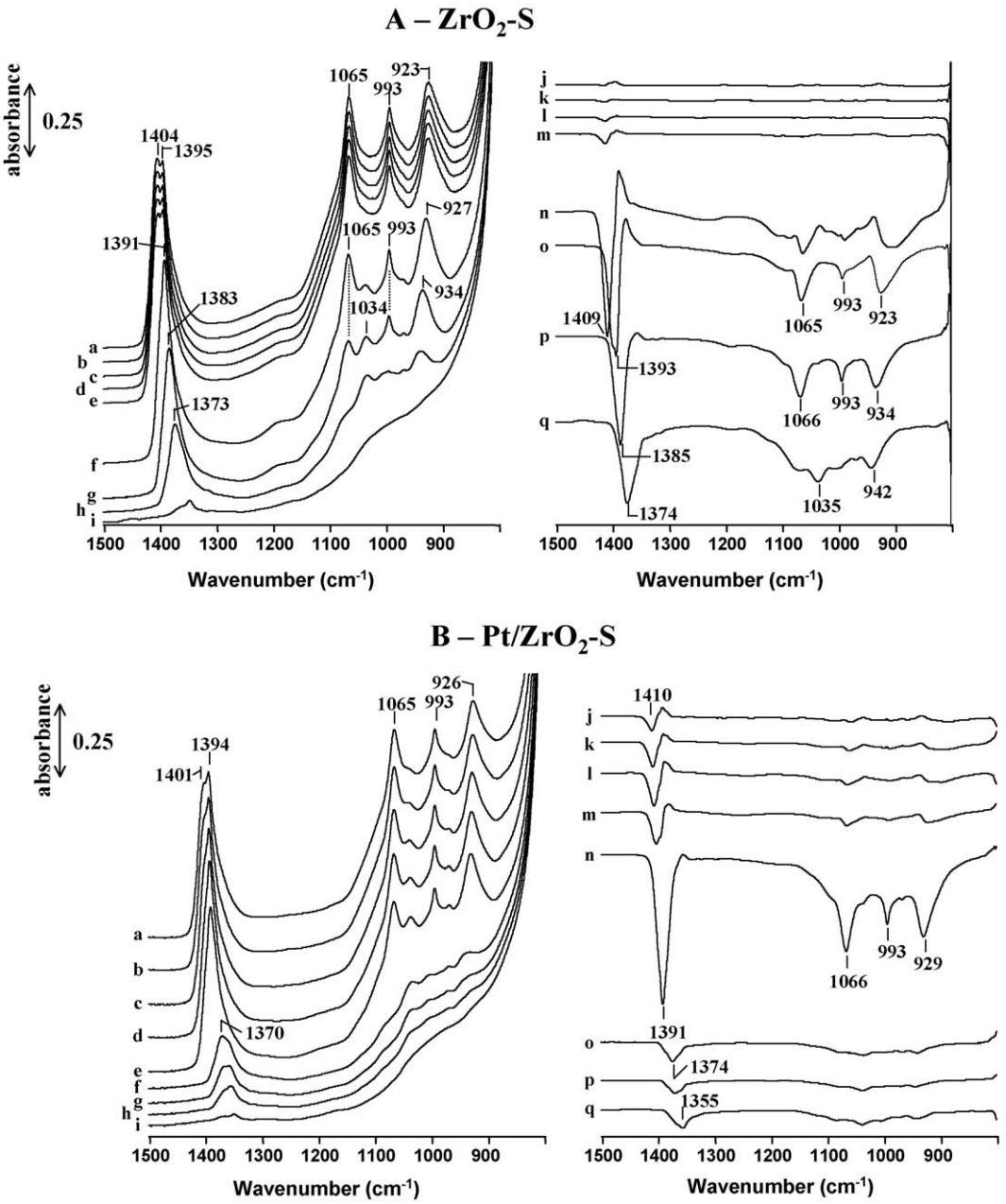

Fig. 7. IR spectra of (A) ZrO_2, (B) Pt/ZrO_2 recorded after (a) sulfation at 723 K by SO_2 (600 μmol g^{-1}) and O_2, then heated under H_2 (30 min) at (b) 323, (c) 423, (d) 523, (e) 623, (f) 723 K (30 min), (g) 723 K (1 h), (h) 723 K (2 h), (i) 723 K (12 h). An evacuation at 723 K is performed for each temperature. Spectra of subtraction (j) b–a, (k) c–b, ... and (q) i–h.

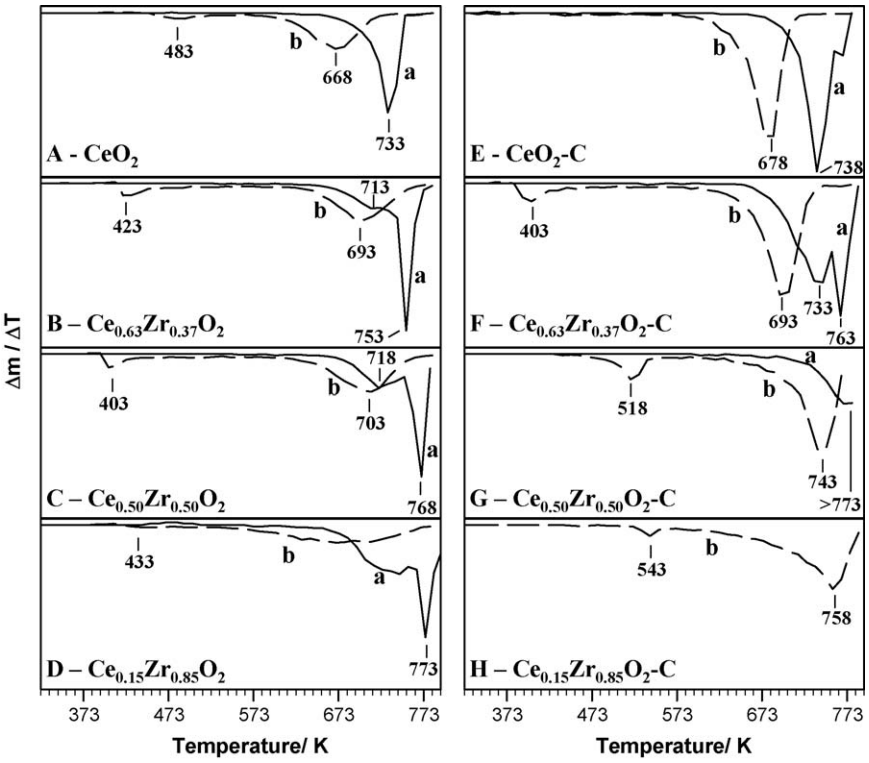

Fig. 8. Derivative of weight variation curves depicted Fig. 6: (a) oxides without Pt, (b) oxides with Pt.

H_2 than the other surface sulfates. The signal associated with the sulfate and pyrosulfate species was essentially entirely removed by the reduction at 723 K (spectrum i). The temperature range of sulfate reduction on ZrO_2–S observed in this work is in agreement with those reported in the literature [14].

3.2.2. Reduction of Pt/ZrO_2–S

The mass loss associated with the Pt/ZrO_2–S sample heated (0.5 K min^{-1}) under hydrogen ($P \sim 13.3$ kPa) from 300 K to 773 K started near 540 K and finished at 773 K (Fig. 6Ce). The platinum favored sulfate reduction at lower temperature as compared to the case of the corresponding Pt-free sample by about 90 K.

IR experiment relating to Pt/ZrO_2–S reduction versus temperature is presented in Fig. 7B. An important decrease of the intensity due to $\nu_{S=O}$ in the range 1420–1350 cm^{-1} is observed in the case of the treatment at 723 K (Fig. 7Bf and n). Results regarding ZrO_2–S also indicated that sulfate reduction took place at the same temperature. However, the sulfate band intensity decreased faster in the presence of Pt: only 30 min at 723 K were necessary to eliminate the majority of the sulfate species (spectrum f), while 2 h were required for the Pt-free sample (spectrum h). More, a decrease of the intensity of 1410 cm^{-1} band assigned to pyrosulfates at 423, 523 and 623 K (spectra c, d, e and k, l, m) was observed in the presence of Pt. No modification of the spectra was observed for the sample without platinum at the same temperatures.

Although the reduction of sulfate species is mainly observed at 723 K on both ZrO_2–S and Pt/ZrO_2–S, a positive effect of platinum can yet be expected. This effect of platinum on sulfate reduction has been described before [10,15,23–28]: H_2 is dissociated on platinum to form hydrogen atoms, which migrates from the metal to the ZrO_2 (spillover of hydrogen) and favors the reduction of sulfate. As a matter of fact, the decrease of $\nu_{S=O}$ bands between 423 and 623 K on Pt/ZrO_2 observed here is mainly due to the reduction of sulfate species located in the neighborhood of platinum particles.

3.2.3. Reduction of $Ce_xZr_{1-x}O_2$–S

3.2.3.1. Effect of the mixed oxide composition. The study of the composition effect for mixed oxides has been carried out by comparing curves of weight variation of samples calcined at 773 K without Pt (Fig. 6A) and their derivatives (Fig. 8). The mass variations for $Ce_{0.63}Zr_{0.37}O_2$–S, $Ce_{0.50}Zr_{0.50}O_2$–S and $Ce_{0.15}Zr_{0.85}O_2$–S sulfated samples recorded during the treatment under hydrogen versus temperature are represented on curves b, c and d, depicted in Fig. 6A, respectively. For all these curves, the beginning of mass loss is near 630 K, similarly to the case of CeO_2. However, we note that the higher the amount of zirconium, the more the curves are shifted towards higher temperatures. The effect of zirconium addition is easier to be observed from derivatives (Fig. 8). The maximum of mass loss is located at 733, 753, 768 and 773 K for CeO_2, $Ce_{0.63}Zr_{0.37}O_2$, $Ce_{0.50}Zr_{0.50}O_2$ and $Ce_{0.15}Zr_{0.85}O_2$ catalysts, respectively. In the case of mixed oxides, a weak mass loss around 715 K can be observed before the main reduction peak.

On infrared spectra (not shown) of sulfated Ce-containing samples reduced at 773 K by H_2 we observe that (i) no bands appears in the 1500–800 cm^{-1} region indicating the total reduction of sulfate species (both surface and bulk-like), and (ii) a band located at ~2113 cm^{-1} which indicates that the ceria was reduced [29].

The mixed oxide mass loss calculated after H_2 treatment and evacuation at 773 K (Table 2, m_1–m_2) are clearly higher than the mass corresponding to sulfate species (m_1) only. The additional mass loss ($m_2 < 0$) is therefore probably due to the reduction of the oxide. The addition of Zr into ceria was actually shown to increase the reducibility of CeO_2 [30–32].

3.2.3.2. Effect of Pt on Pt/$Ce_xZr_{1-x}O_2$–S reduction. The shape of the gravimetric curves obtained for the mixed oxides Pt/$Ce_{0.63}Zr_{0.37}O_2$, Pt/$Ce_{0.50}Zr_{0.50}O_2$ and Pt/$Ce_{0.15}Zr_{0.85}O_2$ (Fig. 6C) are similar to that of the Pt/CeO_2 (Fig. 6Ca): the mass loss occurs in two steps. To explain these two steps, an infrared experiment was carried out to

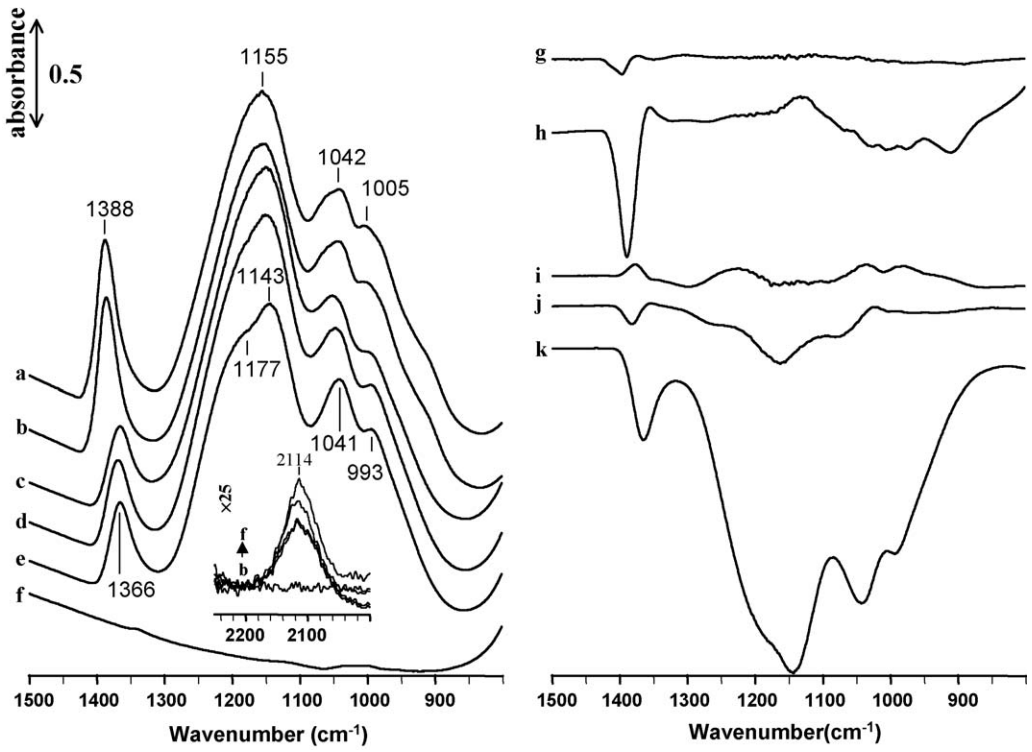

Fig. 9. A: IR spectra of $Pt/Ce_{0.50}Zr_{0.50}O_2$ recorded after (a) sulfation at 673 K by SO_2 (600 μmol g^{-1}) and O_2, then heated under H_2 (30 min) at (b) 323, (c) 423, (d) 523, (e) 623, (f) 723 K and evacuated at the same temperature for each step. Spectra of subtraction (g) b–a, (h) c–b, (i) d–c, (j) e–d and (k) f–e.

investigate the reducibility of sulfate formed on $Pt/Ce_{0.50}Zr_{0.50}O_2$ (Fig. 9). The bands at 1388 and 1155 cm^{-1} present on spectrum a of the sulfated sample are due to surface and bulk-like sulfate species, respectively. The evolution of the spectra versus temperature occurs in two steps as in the case of the gravimetric curve (Fig. 6Cc). The first one, at low temperature (about 423 K—spectrum c), leads to the partial reduction of both surface sulfate species (decrease of the intensity of the 1388 cm^{-1} band) and some of the cerium cations (as indicated by the presence of the band at 2114 cm^{-1}, see inset Fig. 9). No modification of spectrum d recorded at 523 K is noted with respect to spectrum c. The second phenomenon, at high temperature (623–723 K) is the result of the reduction of both surface and bulk-like sulfates (complete elimination of bands characteristics of sulfate species in the 1500–900 cm^{-1} range) and the increasing of sample reduction.

By studying derivatives (Fig. 8), we note that the two steps take place at different temperatures according to the oxide composition. For the first low temperature step, maxima are located at 483, 423, 403 and 433 K for Pt/CeO_2, $Pt/Ce_{0.63}Zr_{0.37}O_2$, $Pt/Ce_{0.50}Zr_{0.50}O_2$ and $Pt/Ce_{0.15}Zr_{0.85}O_2$, respectively. The Zr addition favors the mass loss at lower temperature, therefore the partial reduction of both surface sulfate species and oxide. The opposite trends are obtained for the high temperature peak: the higher the Zr content, the higher the reduction temperature (668, 693 and 703 K for Pt/CeO_2, $Pt/Ce_{0.63}Zr_{0.37}O_2$ and $Pt/Ce_{0.50}Zr_{0.50}O_2$, respectively), excepted for the $Pt/Ce_{0.15}Zr_{0.85}O_2$ mixed oxide (for which a broad ill-defined peak is observed). The temperature of this second step is lowered by about 60 K in presence of platinum, whatever the oxide composition (pure or mixed). The deleterious effect on the reduction induced by the Zr doping reported above for Pt-free samples is also observed for Pt/catalysts.

Concerning the mass loss, it is not markedly affected by the Pt addition (Table 2, m_2 and m_2–m_1) and therefore the final reduction state of sulfated samples with and without Pt is essentially the same after a treatment at 773 K under H_2.

3.2.3.3. Ageing effect. The mechanism of sulfate reduction by H_2 for aged samples (calcined at 1173 K) is similar to that described above for the catalysts calcined at 773 K. The effect of the sample ageing was estimated mostly from the analysis of the thermogravimetric results, considering both the curves of weight variation (Fig. 6B and D) and its first derivative (Fig. 8). The shape of the weight loss curves corresponding to the aged catalysts is very similar to that of the high surface area samples: reduction occurs in one step for oxides without Pt and in two steps for platinum-containing catalysts. For samples without Pt, maxima of mass variation are pointed at 738, 763, and >773 K for CeO_2–C, $Ce_{0.63}Zr_{0.37}O_2$–C and $Ce_{0.50}Zr_{0.50}O_2$–C and for samples with Pt, at 678, 693, 743 and 758 K for Pt/CeO_2–C, $Pt/Ce_{0.63}Zr_{0.37}O_2$–C, $Pt/Ce_{0.50}Zr_{0.50}O_2$–C and $Pt/Ce_{0.15}Zr_{0.85}O_2$–C. Similarly to the case of the samples calcined at 773 K, the reduction temperature of bulk-like species increases with the zirconium amount in the case of the materials calcined at 1173 K. The reduction temperature of the latter samples was similar or somewhat higher.

3.2.4. Sulfur storage by reduction of sulfate species

Following the reduction of sulfated samples by hydrogen at 773 K, dioxygen was introduced in the thermobalance at 673 K with the aim to reoxidize the sample. The weight of all the Ce-based samples increased (Fig. 6, Table 2 (m_3)). Similar experiments made in the infrared cell led to both the appearance of the bands due to the sulfate species and the complete elimination of band around 2112 cm^{-1} whatever the oxide composition (Fig. 10). This last observation shows that the oxides were completely reoxidized by a treatment with oxygen at 673 K. The reappearance of sulfate species indicates that a fraction of those was converted to a sulfide or oxysulfide phase during the H_2 treatment [11,33]. We have previously confirmed the Pt poisoning by sulfur via the study of CO adsorption on a Pt/CeO_2 sample before sulfation and after sulfation and reduction [10].

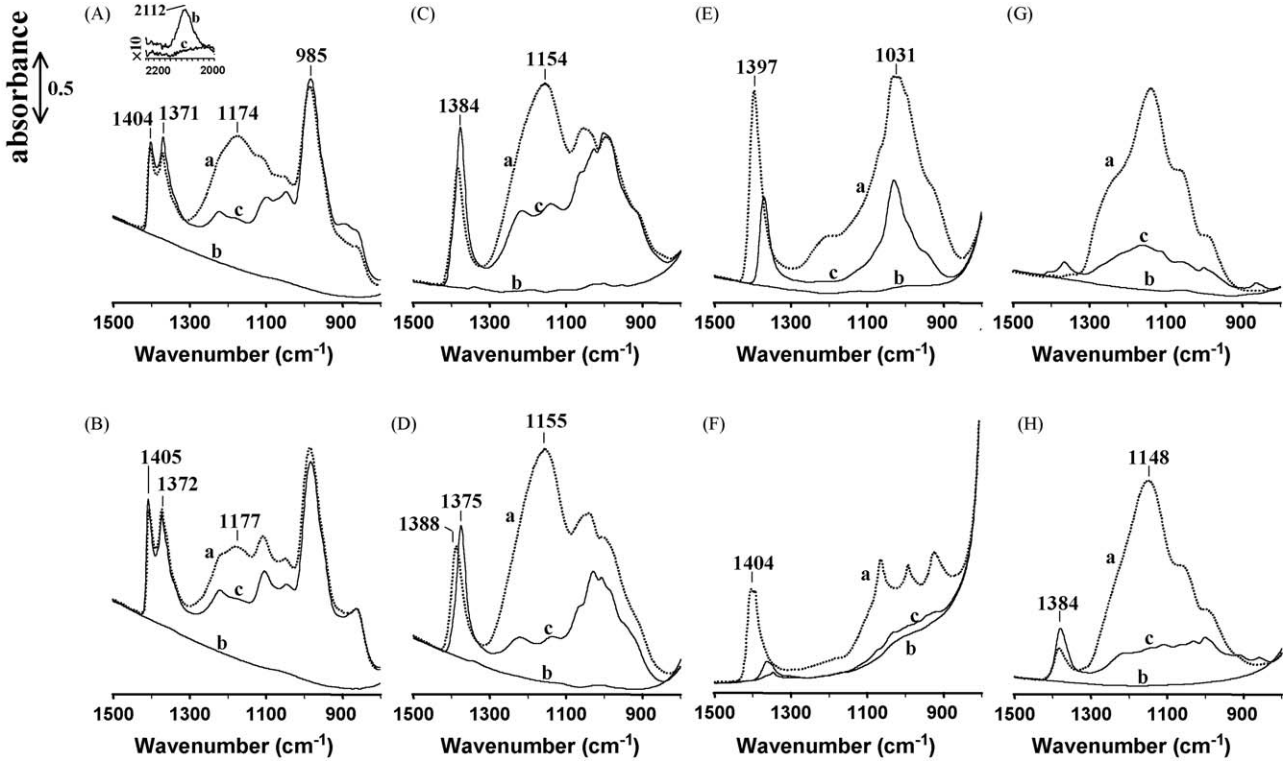

Fig. 10. IR spectra recorded after (a) sulfation at 723 K by SO_2 (600 μmol g^{-1}) and O_2, then (b) heated under H_2 and evacuated at 723 K and finally (c) oxidized at 673 K. (A) CeO_2, (B) Pt/CeO_2, (C) $Ce_{0.63}Zr_{0.37}O_2$, (D) $Ce_{0.50}Zr_{0.50}O_2$, (E) $Ce_{0.15}Zr_{0.85}O_2$, (F) ZrO_2, (G) Pt/CeO_2–C, (H) $Pt/Ce_{0.63}Zr_{0.37}O_2$–C.

The evaluation of the level of sulfur storage obtained on the sulfated samples reduced by hydrogen at 773 K was derived from the thermogravimetric results reported in Table 2. The mass variation of activated samples (a), then (b) sulfated by SO_2 with O_2 at 673 K, then (c) treated by H_2 at 773 K and finally (d) oxidized by O_2 at 673 K are reported in Fig. 11. The concentration of sulfur stored was calculated by considering that O_2 addition led to the complete oxidation of both oxide and sulfur (into sulfate). In these conditions, the amount of sulfur stored on sample (m_S) is given by

$$m_S\ (\mathrm{mg\,g^{-1}}) = \frac{m_3}{M_{SO_3}} \times M_S \quad (1)$$

or

$$m_S\ (\mu\mathrm{mol\,g^{-1}}) = \frac{m_3}{M_{SO_3}} \times 10^3 \quad (2)$$

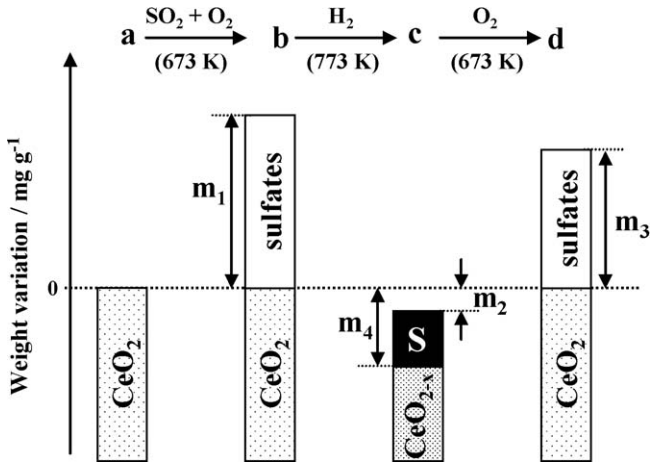

Fig. 11. Schematic representation on weight variation during thermogravimetric measurements of sulfated samples then reduced and finally re-oxidized.

with M_S = 32 g mol^{-1}, atomic weight of sulfur, M_{SO_3} = 80 g mol^{-1}, molecular weight of SO_3, m_3 = weight of sulfate formed by re-oxidation (see Table 2).

The calculated amount of sulfur stored for all samples is reported in Table 2. These data indicate that (i) the higher the Zr content, the smaller the amount of sulfur stored; (ii) the addition of platinum, at least for the loading used here (0.5 wt%), did not modify the sulfur loading and (iii) the aged catalysts exhibited a significantly lower concentration of stored sulfur. Infrared spectra of CeO_2, Pt/CeO_2, $Ce_{0.63}Zr_{0.37}O_2$, $Ce_{0.50}Zr_{0.50}O_2$, Pt/CeO_2–C and $Pt/Ce_{0.63}Zr_{0.37}O_2$–C are reported in Fig. 10A, B, C, D, F and G, respectively. These data show that surface sulfate species are mainly formed following the sample re-oxidation. The comparison of the various oxides (Table 1) reveals that the presence of platinum did not modify the specific surface areas. On the contrary, the ageing at 1173 K strongly decreased the specific surface area. The amount of stored sulfur versus the surface area of catalysts is reported in Fig. 12. A linear relation is clearly observed, particularly in the case of high surface area samples. It can be concluded that the stored sulfur content is proportional to the specific surface area of samples. The values corresponding to mixed oxides $Ce_{0.15}Zr_{0.85}O_2$, rich in Zr, are below those observed for the catalysts having a higher Ce content. However, a linear relation of sulfur stored versus specific surface area might also be observed for the $Ce_{0.15}Zr_{0.85}O_2$ mixed oxides but with a different slope. On the other hand, values for rich Ce-content mixed oxides, calcined at 1173 K, are located above the line. In the case of ZrO_2, some authors consider that no sulfur remains after sulfate reduction with H_2 [23]. Others have proposed that 50% of sulfur was kept on the surface [28]. Bands due to sulfate species appear in Fig. 10F but their intensities are very low. We estimated that the amount of sulfate was negligible (<20 μmol g^{-1}) by measuring both the intensity of the infrared bands of the corresponding sulfate species and sample weight changes.

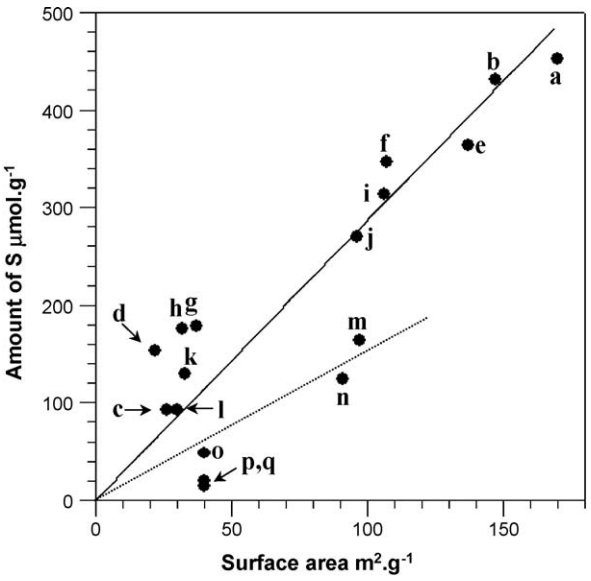

Fig. 12. Amount of sulfur storage on sulfated samples treated under hydrogen at 773 K versus specific surface area: (a) CeO_2, (b) Pt/CeO_2, (c) CeO_2–C, (d) Pt/CeO_2–C, (e) $Ce_{0.63}Zr_{0.37}O_2$, (f) $Pt/Ce_{0.63}Zr_{0.37}O_2$, (g) $Ce_{0.63}Zr_{0.37}O_2$–C, (h) $Pt/Ce_{0.63}Zr_{0.37}O_2$–C, (i) $Ce_{0.50}Zr_{0.50}O_2$, (j) $Pt/Ce_{0.50}Zr_{0.50}O_2$, (k) $Ce_{0.50}Zr_{0.50}O_2$–C, (l) $Pt/Ce_{0.50}Zr_{0.50}O_2$–C, (m) $Ce_{0.15}Zr_{0.85}O_2$, (n) $Pt/Ce_{0.15}Zr_{0.85}O_2$, (o) $Pt/Ce_{0.15}Zr_{0.85}O_2$–C, (p) ZrO_2 and (q) Pt/ZrO_2.

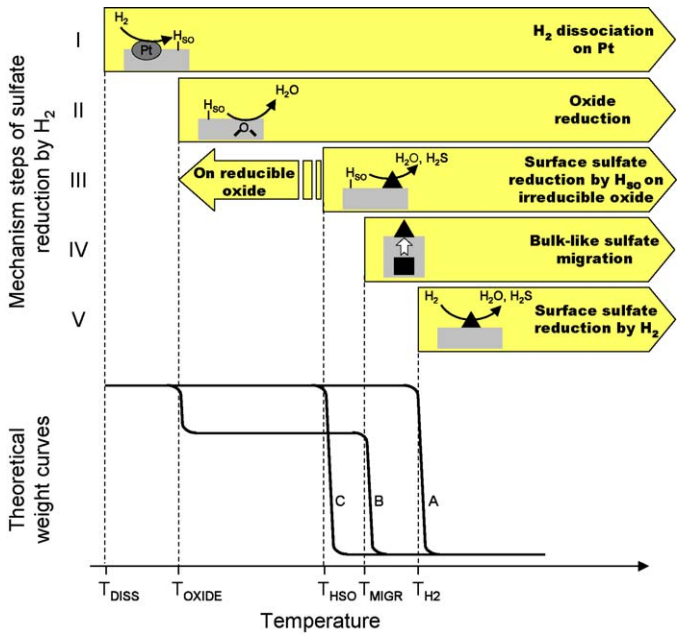

Fig. 13. Schematic representation of the proposed mechanism of reduction of sulfates by H_2. Top part: main steps of the mechanism. H_{SO}—atomic hydrogen formed by the dissociation of H_2: black triangle, surface sulfate; black square, bulk-like sulfate. Bottom part: theoretical weight variation of sulfated samples treated under H_2 versus temperature. A: platinum free sample, B: reducible sample with platinum, C: irreducible sample with platinum. Temperature of: T_{DISS}, H_2 dissociation on Pt; T_{OXIDE}, oxide reduction; T_{HSO}, surface sulfate reduction by H_{SO}; T_{MIGR}, bulk-like sulfate migration; T_{H2}, surface sulfate reduction by H_2.

3.2.5. OSC of sulfated Ce-containing samples

The OSC (redox capacity) of sulfated Ce-based catalysts at 773 K was assessed using thermogravimetric measurement. As is shown in Fig. 11, the level of oxygen (m_4) released during the reduction of the oxide is given by

$$m_4\ (\mathrm{mg\,m^{-1}}) = m_S - m_2 \quad (3)$$

or

$$m_4\ (\mathrm{mmol\,g^{-1}}) = \frac{m_S - m_2}{M_O} \times 10^3 \quad (4)$$

with M_O = 16 g mol^{-1}, atomic weight of oxygen, m_S and m_2 in mg (see Table 2).

The evaluation of the OSC at 773 K is 837, 1254, 1295 and 514 µmol g^{-1} of atomic oxygen for CeO_2, $Ce_{0.63}Zr_{0.37}O_2$, $Ce_{0.50}Zr_{0.50}O_2$ and $Ce_{0.15}Zr_{0.85}O_2$, respectively. The OSC of the ceria–zirconia materials has been assessed using three methods in parallel: temperature programmed reduction, FT-IR measurements of methanol and Faraday microbalance over similar materials [34]. The OSC is higher for ceria–zirconia mixed oxides (excepted for $Ce_{0.15}Zr_{0.85}O_2$) than it is for pure ceria and is practically the same for Zr contents between 20% and 50%. Similar conclusions could be proposed in our study in the case of the sulfated samples; however, the OSC reported in Table 2 are higher than those reported in reference [34]. This higher OSC observed here could possibly be due to the replacement of some oxygen with S in the sample lattice (i.e. formation of an oxysulfide), resulting in a higher effective release of oxygen in the case of the sulfated materials. The OSC of sulfated samples with and without Pt determined by the thermobalance at 773 K is very similar on both fresh and aged oxides. However, the OSC of the aged samples is much lower than that of the fresh materials (Table 2). Therefore the thermogravimetric measurements appears to be a good method for the evaluation of OSC of sulfated ceria–zirconia mixed oxides.

3.2.6. Mechanisms of sulfate reduction by H_2

Taking into account the above reported results, a mechanism for sulfate reduction by hydrogen including five main steps can be proposed (see scheme in Fig. 13). An exchange mechanism between surface and bulk-like sulfate species would prevail (step IV). The elimination of sulfate species from the surface (for example through reduction with H_2) leads to a surface-bulk unbalance, which is then corrected by sulfate migration from the bulk to the surface. However, this migration might occur only above a threshold temperature (T_{MIGR}), evaluated to be around 673 K. The value of T_{MIGR} is related to the nature of the oxide. In particular, the higher the Zr content in CeO_2–ZrO_2 mixed oxides, the greater the T_{MIGR}.

When the sample is reducible like CeO_2 or CeO_2–ZrO_2 compounds, the reduction of the sulfate and oxide phases occurs concomitantly. During this study, various levels of reducibilities of the sulfate species was observed, depending on the nature of the oxide used, in particularly between pure ceria and zirconia. CeO_2 is easily reduced in the presence of reducing agents such as H_2, while ZrO_2 is irreducible. We suggest that the redox properties play an important part in the sulfate reduction. However, in the case of the samples free of Pt, the sulfate reduction occurs in the 673–773 K temperature range, having no correlation with the reducibility of the samples. For these catalysts free of Pt, we propose that the reduction is connected with the own reducibility of the surface sulfate species, probably with a direct reaction of H_2 on these adsorbates, i.e. without the formation of intermediate species, such as hydroxyl groups (step V and theoretical curve A, Fig. 13). In fact these species (arising from a heterolytic dissociation process) can be formed at temperatures as low as 373 K, much lower than those observed for sulfate reduction [35]. Experimental results reveal that Pt addition favors sulfate reduction by H_2. In this case, a homolytic dissociation of molecular hydrogen on the metal could be hypothesized, which leads to the formation of atomic hydrogen, more reactive towards surface species, thus easier reduced (step I). The platinum effect is variable according to the nature of samples. Two situations can be considered:

3.2.6.1. Mechanism of sulfate reduction by H_2 on irreducible oxide (ZrO_2). The reduction of sulfate species on ZrO_2 takes place at a lower temperature in presence of Pt, the temperature shift being about 100 K. The promoting effect of platinum is most likely due to favor the dissociation of H_2, the atomic hydrogen formed (noted H_{SO}) migrating then to the ZrO_2. The H_{SO} (more active than H_2) induces sulfate reduction at lower temperature (step III and theoretical curve C, Fig. 13).

3.2.6.2. Mechanism of sulfate reduction by H_2 on reducible oxides (CeO_2 and CeO_2–ZrO_2). The platinum effect on sulfate reduction is much clearer in the case of CeO_2 than in that of ZrO_2. Other factors than hydrogen dissociation on Pt should be considered to explain this result. In particular, the CeO_2 reduction is concomitant to the surface sulfate reduction. We suggest that the sulfate reduction mechanism on ceria involves the redox properties of the sample (step II). The first step is the H_2 dissociation on platinum surface to form H_{SO}, which spills over the ceria surface (step I). The action of H_{SO} leads to the reduction of ceria and a part of surface sulfate species (step III). In the case of CeO_2, the reduction occurs at a temperature lower than T_{MIGR}. Therefore, two distinct steps are observed (theoretical curve B, Fig. 13). The second step consists in the reduction of bulk-like sulfate species following their migration from bulk to the surface. In this mechanism, in the presence of Pt, the formation of surface sulfate species supported on reduced ceria probably takes place. We were not been able to observe experimentally these species, probably due to their very high reactivity with H_{SO}.

4. Conclusions

The spectral analysis of mixed oxides $Ce_xZr_{1-x}O_2$ sulfated by 600 μmol g^{-1} of SO_2 in an excess of O_2 at 673 K highlighted the presence of both surface and bulk-like sulfate species. The cerium centers retains an ability to form sulfate ionic species even in the presence of high Zr content. The concentration of ionic sulfates is lowest for the Zr-rich oxide $Ce_{0.15}Zr_{0.85}O_2$. The molar ratio between ionic and surface sulfate species is higher in the case of aged oxides (which also possess a low specific surface area). Consequently, the proportion of the two species (surface and bulk-like) is directly linked to the specific surface area of the sample. The thermogravimetric study of the sulfation versus temperature reveals that three factors mainly intervene in the sulfate migration process from surface to bulk. Firstly, the specific surface area of the oxide, secondly, the presence of platinum, which favors SO_2 oxidation into SO_3 and, finally, the zirconium addition to CeO_2, which hinders sulfation.

The study of sulfate reduction by H_2 on simple ceria or zirconia oxides and on various mixed oxides $Ce_xZr_{1-x}O_2$ (calcined at low or high temperature, with or without platinum) reveals that:

1. The reduction of sulfate formed on CeO_2 occurs in the 673–773 K range for all sulfate species (surface and bulk-like);
2. Sulfate reducibility is more difficult in the case of the catalysts calcined at high temperature;
3. Sulfate reduction occurs at the oxide surface, then bulk-like species migrate towards the surface to replace surface sulfate species eliminated by the reduction. In this interpretation, bulk-like species can be considered like a reservoir;
4. The higher the Zr-content for $Ce_xZr_{1-x}O_2$ mixed oxides, the higher the reduction temperature of sulfates;
5. The addition of Pt favors the reduction of sulfates by H_2, two steps being observed. The first, at low temperature (423–523 K), relates to the partial reduction of both oxide and surface sulfate species. The reduction temperature decreases with the increase of the Zr-content ($Zr < 50\%$). The second step, at higher temperature (623–723 K), corresponds to the complete reduction of sulfate species (surface and bulk-like ones). The addition of zirconium increases the temperature at which this second step occurs, probably by making the sulfate migration more difficult.
6. Sulfur is stored at the oxide surface probably in the form of oxysulfide of cerium as well as on platinum [10]. The amount of stored sulfur is closely linked to the specific surface area of the sample. Platinum does not affect noticeably this sulfur-storage capacity and high Zr-content inhibits sulfur formation.
7. The oxide reduction is always concomitant to that of sulfates.

We have clearly shown that thermogravimetric measurements can be a successful method for the evaluation of OSC of sulfated ceria–zirconia mixed oxides.

References

[1] H.S. Gandhi, A.G. Piken, M. Shelef, R.G. Delesh, SAE Technical Paper 760201 (1976).
[2] A. Trovarelli, Catal. Rev.-Eng. 38 (1996) 439.
[3] M. Pijolat, M. Prin, M. Soustelle, O. Touret, P. Nortier, J. Chem. Soc., Faraday Trans. 91 (1995) 3941.
[4] J.R. González-Velasco, M.A. Gutiérrez-Ortiz, J.-L. Marc, Juan A. Botas, M.P.r. González-Marcos, G. Blanchard, Appl. Catal. B: Environ. 22 (1999) 167.
[5] P. Fornasiero, G. Balducci, R. Di Monte, J. Kašpar, V. Sergo, G. Gubitosa, A. Ferrero, M. Graziani, J. Catal. 164 (1996) 173.
[6] Y.J. Mergler, A. van Aalst, J. van Delft, B.E. Nieuwenhuys, Appl. Catal. B: Environ. 10 (1996) 245.
[7] R. Burch, J.P. Breen, F.C. Meunier, Appl. Catal. B: Environ. 39 (2002) 283.
[8] C.N. Costa, P.G. Savva, J.L.G. Fierro, A.M. Efstathiou, Appl. Catal. B: Environ. 75 (2007) 147.
[9] M. Waqif, P. Bazin, O. Saur, J.C. Lavalley, G. Blanchard, O. Touret, Appl. Catal. B: Environ. 13 (1997) 265.
[10] P. Bazin, O. Saur, J.C. Lavalley, G. Blanchard, V. Visciglio, O. Touret, Appl. Catal. B: Environ. 11 (1997) 193.
[11] P. Bazin, O. Saur, J.C. Lavalley, A.M. Le Govic, G. Blanchard, Stud. Surf. Sci. Catal. 116 (1998) 571.
[12] T. Luo, R.J. Gorte, Appl. Catal. B: Environ. 53 (2004) 77.
[13] G. Colón, M. Pijolat, F. Valdivieso, H. Vidal, J. Kašpar, E. Finocchio, M. Daturi, C. Binet, J.C. Lavalley, J. Chem. Soc., Faraday Trans. 94 (1998) 3717.
[14] M. Bensitel, O. Saur, J.C. Lavalley, B.A. Morrow, Mater. Chem. Phys. 19 (1988) 147.
[15] A. Melchor, E. Garbowski, M.V. Mathieu, M. Primet, React. Kinet. Catal. Lett. 29 (1985) 371.
[16] D. Martin, D. Duprez, J. Phys. Chem. 100 (1996) 9429.
[17] A. Galdikas, C. Descorme, D. Duprez, Solid State Ionics 166 (2004) 147.
[18] A. Galdikas, D. Duprez, C. Descorme, Appl. Surf. Sci. 236 (2004) 342.
[19] C. Morterra, G. Cerrato, F. Pinna, M. Signoretto, G. Strukul, J. Catal. 149 (1994) 181.
[20] F. Pinna, M. Signoretto, G. Strukul, G. Cerrato, C. Morterra, Catal. Lett. 26 (1994) 339.
[21] C. Morterra, G. Cerrato, F. Pinna, M. Signoretto, J. Phys. Chem. 98 (1994) 12373.
[22] M. Signoretto, F. Pinna, G. Strukul, C. Morterra, Catal. Lett. 36 (1996) 129.
[23] R. Le Van Mao, S. Xiao, T. Si Le, Catal. Lett. 35 (1995) 107.
[24] A. Li-Dun, D. You Quan, Appl. Catal. 66 (1990) 219.
[25] K. Ebitani, T. Tanabé, H. Hattori, Appl. Catal. A 102 (1993) 79.
[26] A. Dicko, X. Song, A. Adnot, A. Sayari, J. Catal. 150 (1994) 254.
[27] R. Srinivasan, R.A. Keogh, D.R. Milburn, B.H. Davis, J. Catal. 153 (1995) 123.
[28] B.Q. Xu, W.M.H. Sachtler, J. Catal. 167 (1997) 224.
[29] C. Binet, A. Badri, J.C. Lavalley, J. Phys. Chem. 98 (1994) 6392.
[30] P. Fornasiero, R. Di Monte, G.R. Rao, J. Kaspar, S. Meriani, A. Trovarelli, M. Graziani, J. Catal. 151 (1995) 168.
[31] T. Murota, T. Hagesawa, S. Aozasa, H. Matsui, M. Motoyama, J. Alloy Compd. 193 (1993) 298.
[32] C. Binet, M. Daturi, Catal. Today 70 (2001) 155.
[33] T. Luo, J.M. Vohs, R.J. Gorte, J. Catal. 210 (2002) 393.
[34] M. Daturi, E. Finocchio, C. Binet, J.C. Lavalley, F. Fally, V. Perrichon, H. Vidal, N. Hichey, J. Kaspar, J. Phys. Chem. B 104 (2000) 9186.
[35] M. Daturi, E. Finocchio, C. Binet, J.C. Lavalley, F. Fally, V. Perrichon, J. Phys. Chem. B 103 (1999) 4884.